DESIGN, CHARACTERIZATION AND IN VIVO EVALUATION OF NANOSTRUCTURED LIPID CARRIERS (NLC) AS A NEW DRUG DELIVERY SYSTEM FOR RANOLAZINE ORAL ADMINISTRATION FOR HYPERTENSION

Abdul Sayeed Khan[a]*, Bhupen Chandra Behera[b]

Article History: **Received:** 03.12.2022 **Revised:**15.01.2023 **Accepted:** 20.02.2023

Abstract: Low solubility and permeability of raolazine (RZ) result in restricted and changeable bioavailability; less stability makes it challenging to create stable aqueous liquid formulations; low dosage makes it challenging to achieve homogenous medication distribution. This study set out to determine whether a plan based on the creation of nanostructured lipid carriers (NLC) as a novel oral formulation of RZ with enhanced therapeutic efficacy was effective. Solid and liquid lipids, as well as surfactant produced by hot homogenization and ultrasonication, were used to design and create nanostructured lipid carriers (NLCs). An strategy based on quality by design (QbD) was used to optimise the formulation. Through the use of a central composite design, three variables—total lipid concentration, surfactant concentration, and sonication time—were optimised to determine how they would affect the critical quality attributes (CQAs) of size (nm), entrapment efficiency (%), and in vitro drug release, which were discovered to be 126.495.46nm, 85.341.29%, and 92.370.31%, respectively, after 24 hours. The oral bioavailability of the optimised nanostructured lipid carrier increased by 4.207 and 1.907 times, respectively, with and without cycloheximide (a lymphatic transport inhibitor). As a result, systematic quality through design integration increased the gut permeability and probable solubilization destiny (dynamic lipolysis) of RZ-NLC, which further improved the lymphatic absorption and biodistribution of medication, thus promising its in vivo prospect and clinical efficacy. Therefore, it can be stated that the "Central composite design" was effectively used to optimise the RZ loaded NLCs, which improved the oral bioavailability of ranolazine in Wistar rats and calls for future research.

Keywords: Ranolazine, Central composite Design, Homogenization, Ultra-sonication, pharmacokinetics, bioavailability.

[a]. Department of Pharmaceutics, The Pharmaceutical College, Barpali, Bargarh-768029, Odisha, India.
[b]. Department of Pharmaceutics, Kanak Manjari Institute of Pharmaceutical Sciences, Rourkela-769015, Odisha, India.

***Corresponding Author**

E-mail:sayeed78khan@gmail.com, prof.bcbehera@gmail.com

DOI: 10.31838/ecb/2023.12.2.003

INTRODUCTION

In contrast to being a disease in and of itself, hypertension, which is currently a global epidemic, is a significant risk factor for major cardiovascular illnesses such as causes of death include cardiac arrest, stroke, congestive heart failure, and peripheral artery disease. [1, 2]. Angina pectoris is a frequent kind of persistent chest pain caused by inadequate blood flow to the heart (ischemia) or by spasm of the coronary arteries. Medications such as nitrates, beta-blockers, calcium channel blockers, etc., are used to treat angina for symptom alleviation and heart rate control [3, 4]. Anti-ischemic and metabolic capabilities [5, 6] led to ranolazine's (RZ) first approval by the US FDA in 2006. RZ undergoes substantial and complicated biotransformation throughout its 1.4-1.9 h half-life. An t12 of 7 h and an effective dosage of 500–1000 mg twice day characterise its ER formulation [7, 8]. When administered orally, RZ has a limited bioavailability due to the first-pass action, gastrointestinal (GI) discomfort, a high therapeutic dose, and poor absorption. Poor patient compliance [9] is an additional obstacle for the gastrointestinal and immobile patient. There have been no previous attempts to improve patient compliance, and there is only a small amount of information about RZ lipid nanopartciledelivery in the literature. As a result, RZ's unique carrier drug delivery might be a notable way to circumvent these challenges and accomplish regulated drug delivery with generally improved patient compliance thanks to the medication's easy and painless administration. However, researchers have made progress in creating transdermal patches for the administration of various drugs (atenolol, nitro-glycerin, diltiazem, timolol, etc). The most effective method for transdermal administration of RZ into the circulatory system was via nano-vesicular lipid nanoparticles. [10,11].

Attempts have been made to remedy the aforementioned issues with RZ by creating NLCs of RZ with certain additives. NLCs are a popular pharmaceutical preparations because of their many benefits, which include efficient drug encapsulation, biodegradability, biocompatibility, a predictable release profile, and scalability at low cost [12]. To create NLCs, liquid lipids and solid lipids are combined. Over time, a solid lipid nanoparticle can create a perfect crystalline

lattice, leaving less room for the medicine to remain inside and ultimately causing the drug to be expelled. Liquid lipids present in NLCs hinder crystal structure formation, boosting drug entrapment efficiency and decreasing the likelihood of gel formation during storage [13]. Since the loading capacity of lipophilic medications is greater in lipids than in hydrophilic pharmaceuticals, drugs with a elevated log P value are good candidates for NLCs formulation. Therefore, NLCs allow for lymphatic absorption, which avoids hepatic first pass metabolism [14]. In order to enhance the formulation's ability to treat hypertension and heart attacks, we plan to utilise excipients with P-glycoprotein (P-gp) inhibitory activity for drugs that are substrates for P-gpefux. [15].

In the current study, RZ-loaded NLCs using CCD are developed and optimised utilising hot homogenization and ultrasonication. An experimental approach was used to statistically optimise GMS, oleic acid, and surfactant. To improve oral competency, the produced NLC formulations were lyophilized, investigated for screening, and contrasted with commercial formulations. The solid state characterisation, morphological, invitro, in vivo, and physical stability of the improved formulation of RZ-loaded NLCs were also assessed.

MATERIALS AND METHODS

Materials

Alembic Pharmaceutical Limited, an Indian pharmaceutical company, provided us with a free sample of ranolazine. A 500mg Ranolaz tablet was obtained at the drugstore. Glyceryl monostearate lipid was gift sample from SD fine chemicals India. The molecular weight cutoff (MWCO)=12,000-14,000 Da LA 393-1 MT dialysis membrane was acquired from HiMedia in Mumbai, India. Our poloxamers, 188 and 407, came from BASF in Mumbai. The acetonitrile:water used for HPLC analysis was acquired from Merck India Ltd. (Mumbai, India). Experiment reagents were only of AR quality..

Screening of solid lipids

In a glass vial with a flat bottom and screw cover, 5 mg of RZ was ingested, then 100 mg of lipids were added in 5 mg increments. After heating vials in a water bath to a temperature over the solid lipid melting point, they were vortexed. The quantity of solid lipid necessary to dissolve the medication in a molten state was used to assess the solubility of RZ. [16].

Screening of liquid lipids (oils)

In order to test the saturation solubility of RZ in various oils, an excess quantity of the drug in oil (1.02 ml) was kept at 120.3 rpm [17] and 40°C for 24 hours in a water shaker bath. Additionally, the sample was centrifuged for 10 minutes at 10,000 rpm, and the supernatant was collected, filtered, and diluted with methanol. Additionally, it was examined utilising a C18 analytical column and reverse phase high pressure liquid chromatography (RP-HPLC). Acetonitrile and 10 mM phosphate buffer (pH 2.8) (45:55 v/v) made up the optimum mobile phase, which flowed at a rate of 1.2 ml/min. Using a PDA detector, samples of 10 l were examined for the measurement of RZ at 272 nm (max). [18,19].

Screening of surfactant

NLCs were created using a high-shear homogenizer and previously chosen lipids for surfactant screening in order to choose the best surfactant. The surfactant conc (1% w/v) was maintained, and the chosen surfactant's concentration was further tuned. The selection criteria to optimise the surfactant and its conc were particle size, polydispersity index (PDI), zeta potential, and percent encapsulation efficiency (EE). [20].

Preparation of NLCs

High pressure homogenization was used to create NLCs [21,22]. Weighed accurately, the liquid and solid lipids (which included magnetic beads) were then transferred to a beaker. At 60 °C, lipid phase melted. This medication was mixed with an addition to create a homogeneous bulk. Tween 80 and poloxamer 188 were dissolved at 3% in distilled water to form an aqueous phase, and magnetic beads were added to a third beaker. At 60 °C, both the aqueous and lipid phases were heated. Then, aqueous phase was introduced to the beaker of lipid phase that was being stirred by a magnetic device. The RQ-127A/D from Remi, India was then used to apply high shear homogenization to the hot dispersion at a speed of 6,000 revolutions per minute. High pressure homogenization was used on this hot dispersion at varying pressures and cycle counts to get a uniform mixture. (Stansted Fluid Power Ltd. Unit 5, New Horizon, ESSEX CM19 5FN UK). Once the dispersion cooled to room temperature, RZ-NLCs developed. NLCs were purified by soaking them in 300 mL of pure water while being agitated at 300 rpm for 24 hours to dislodge any unentrapped medicine from the surface. The distilled water was replaced after sitting for 12 hours. [23].

Optimization of NLCs

Utilizing the Minitab 18 programme, the Central Composite Design (CCD), a response surface technique design, was used to improve the formulation (Minitab Inc., State College, PA). Total lipid concentration (%), surfactant concentration, and sonication duration are the three variables (X1 to X3) shown in Table 1, Both of these independent variables are influenced by one of three levels (low, medium, and high) (CQAs). CCD metrics such sample size, entrapment efficiency, and drug release rate were used to evaluate each experimental run. The computer created twenty tests with five possible midpoints.**Table 1.** Factors used in experimental design

Independent Variables			
Parameter	**Low (-1)**	**Medium (0)**	**High (+1)**
X1 (%w/v)	1	3	5
X2 (%w/v)	2	3	4
X3 (min)	5	7.5	10
Dependent variables			
Y1 (%)	Maximize		
Y2 (nm)	Minimize		
Y3	Maximize		

Based on the response surface plots, we could anticipate how varying the independent factors would affect the response parameters. [24].

$$Y= b_0+b_1X_1+b_2X_2+b_3X_3+b_{12}X_1X_2+b_{13}X_1X_3+b_{23}X_2X_3+b_{11}X_{12}+B_{22}X_{22}B_{33}X_{32}$$

particle size, extent of expansion (EE), and percent cumulative drug release (CDR) are examples of dependent variables; b0 is an intercept; b1 through b33 are regression coefficients for respective variables; and Y is the response of dependent variable linked with each component level combination. [25].

Characterization of NLC

Particle size, PDI and zeta potential

Dynamic Light Scattering (DLS) was used to physically characterise the lipid dispersions in terms of mean particle size, PDI, and zeta potential (Zetasizer Nano-ZS90, Malvern Instruments, Malvern, UK). To prevent multi-scattering effects, NLCs dispersions were appropriately diluted with bi-distilled water before to testing. The findings of each measurement were performed in triplicate and reported as average values. ± S.D [26].

Drug entrapment efficiency (EE%)

Briefly, 1.5 mL of NLCs dispersion were placed in the upper chamber of a membrane concentrator and centrifuged for 8 min at 4000 g(Cirri et al., 2012). The unentrapped drug collected in the filtrate in the lower chamber was assayed by UV spectroscopy at 272 nm [27]. Entrapment efficiency (% EE) was calculated according to Equation.

$$\% \text{ EE} = \frac{W \text{ intial drug} - W \text{ free drug}}{W \text{ intial drug}} X100$$

Morphological investigation of NLC

At 80 Kv, a "Morgagni 268D transmission electron microscope" (Fei Electron Optics, Eindhoven, Netherlands) was used to investigate the morphology of the negatively stained NLCs dispersion with "phosphotungstic acid" (1%). The generated RZ loaded NLC's morphological properties, including its form and surface structure, were analysed using scanning electron microscopy (Carl Zeiss Evo 18, Germany).

In vitro release: These studies of optimised RZ-NLCs were assessed for 2 hours and 24 hours, respectively, in simulated gastric fluid (SGF) with a pH of 1.2 and simulated intestinal fluid (SIF) with a pH of 7.4 [30, 31]. Briefly, 200 mL of dissolving medium (SGF and SIF) with 1% Tween 80 were poured in each beaker of the dialysis bags containing 1 mL of formulation equivalent to 10 mg of medication. For dissolving media kept at a temperature of 37 °C on a magnetic stirrer, the stirring speed was fixed at 100 rpm [32]. For the purpose of maintaining consistent volume, two millilitres from each aliquot were removed at various time intervals and replaced with the same quantity of dissolving medium. Aliquots were diluted appropriately, and a UV spectrophotometer was used to check for drug content.

Pharmacokinetic study: these studies in rats were analysed [33] after they were given RZ suspension (RZ suspended in 2% CMC) and Ranolazine-NLCs at a dosage of 10 mg/kg using an 18-gauge oral feeding needle. Rats were placed into two groups (n=4), RZ suspension and RZ-NLCs, and fasted overnight with free access to water. All groups received 12 mg/kg of ranolazine-NLCs orally after 1 hour after injection. Through the tail vein, 0.2 mL of blood samples were taken at various time intervals (1, 2, 4, 8, 12 and 24 h) and placed in a microcentrifuge tube containing EDTA. Utilizing the HPLC technique, the drug's plasma concentration was quantified. [34].

Estimation of Ranolazine in plasma

By using solvent extraction and partitioning, RZ in plasma was calculated. In a nutshell, 0.5 mL of acetonitrile was added to 0.2 mL of rat plasma and vortexed for one minute. After adding 1 mL of ethyl acetate and stirring for 1 minute, the liquid was centrifuged at 4000rpm for TEN minutes. The organic layer on top was scraped off into a fresh test tube and evaporated at 502 °C in a nitrogen stream until completely dry. The residue was prepared with 0.2 mL of mobile phase, which is a combination of acetonitrile and water, and then strained through a 0.25-m membrane (50:50). The drug concentration was calculated by injecting 20 L of the reconstituted sample onto the HPLC. [35,36].

Pharmacodynamic study

Rats with artificially elevated blood pressure were used for the preclinical evaluation of the proposed formulation's antihypertensive efficacy. Deoxycorticosterone acetate (DOCA, 5 mg/kg in corn oil) was SC injected every 4th day for II weeks to cause hypertension [14]. Animals receiving DOCA had higher systolic blood pressure. The rat was then secured in the restrainer, and the non-invasive BP device (NIBP 200A; Biopac System, Inc., Goleta, CA) based on the cuff tail approach was used to record the systolic BP in triplicate at intervals of 0, 1, 2, 4, and 8 hours. All of the animals were discovered to be hypertensive after receiving DOCA therapy for two weeks, with mean systolic blood pressure ranging from 161.23 to 171.34mmHg. For experiments on antihypertensive action, the rats were grouped into three of six at random after two weeks. Rats in groups II and III were treated with RZ suspension and RZ-NLCs formulation (10 mg/kg), whereas group I acted as the control group and received normal saline. To assess the effectiveness of the formulation, blood pressure readings were taken again from each group of rats. [36].

Induction of myocardial infarction

Rats were injected with ISO (85millig/kg, i.p.) solutions in normal saline on days 6 and 7 of the experiment to cause MI .

Experimental protocol: 16 Wistar rats in total were utilised in the investigation. Rats were acclimated before being randomly separated into 4 groups, each with 4 rats. As a control, Group I was given 1 mL of regular saline daily for 7 days. Group II functioned as the toxic group and was given ISO (85 mg/kg, i.p.) on the sixth and seventh days in addition to normal saline (1 mL) orally for seven days. Groups III and IV acted as the test groups, receiving RZ suspension and RZ-NLCs at the same dose of 10 mg/kg/day for 7 days, respectively, as well as ISO (85 mg/kg, i.p.) on the sixth and seventh days. [37].

Blood was drawn from each group's rat tail vein twenty-four hours after the last treatment, and the serum was separated and kept for biochemical analysis at 20 °C5 °C. Following the induction of CO2 anaesthesia, hearts were immediately removed and thoroughly cleaned. For transmission electron microscopy, a small slice of heart was fixed in a solution of 2.5% glutaraldehyde and 2% paraformaldehyde in 0.1 M sodium phosphate buffer (pH 7.2). For biochemical calculations, the remaining heart was maintained at 20 °C.

Stability studies of Ranolazine-NLCs under storage

In order to conduct stability experiments on RZ-NLCs, three months of storage at 4 °C were used. Mean particle size, PDI, and zeta potential were measured using DLS. To look for any potential crystallisation, precipitation, or mould growth, visual inspection was also used. Decisions were made in triplicate, with the outcomes given as average values S.D.[39].

Statistical analysis

By utilizing the Graph Pad Prism version 6.0 software, the findings of all the aforementioned investigations were statistically analysed using one-way analysis of variance (ANOVA), followed by the student-Newman-Keuls multiple comparison post-test (San Diego, CA, USA). When p >0.05., the differences were deemed statistically significant.

RESULTS

Selection of liquid lipids

In order to choose the most effective ones, a number of synthetic (Transcutol®HP, CapryolTM 90, LabrafacTMPG, and LabrafilTMLipophile WL1349) and natural (oleic acid, castor, sesame, and peanut oils) liquid lipids were examined for their ability to bind Ranolazine. (Figure 1).

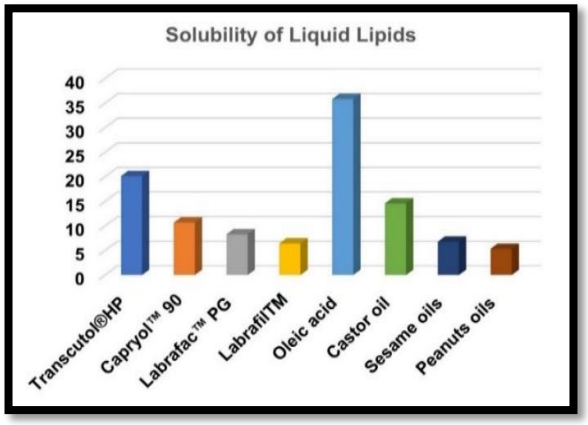

Figure 1: Solubility determination of Liquid Lipids

Solubility studies of RZ in various lipids

Ranolazine's solubilities in glyceryl monostearate, cetyl alcohol, palmitic acid, and stearic acid were assessed for the selection of lipids by measuring the quantity of the medication in each (Figure 2). The values were 5.364±0.076 mg/mL for glycerylmonostearate, 3.169±0.061 mg/mL for cetyl alcohol, 2.95± 0.057 mg/mL for palmitic acid, and 7.349±0.094 mg/mL for stearic acid, respectively.

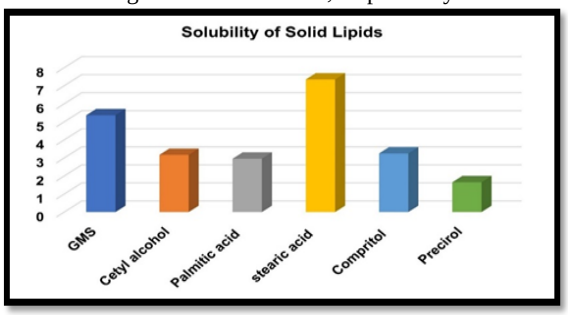

Figure 2: Solubility determination of drug in various solid lipids

Selection of Surfactant

Solubility of Ranolazine in surfactants is given in Figure 3. A The least drug-soluble surfactant helps to keep the drug in the lipid core and strengthens its bond with the lipid matrix. A surfactant exhibiting the least solubility was chosen in order to achieve good nanoparticle stability, high entrapment efficiency, and strong lipid-drug interaction. Soy lecithin, Gelucire, Labrasol 44/14.

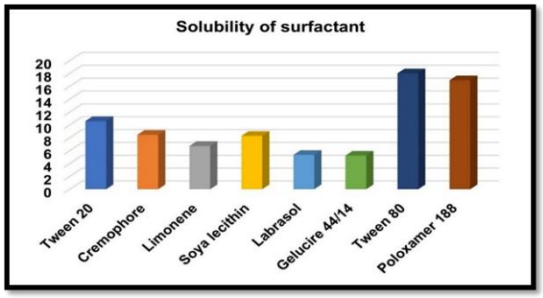

Figure 3: Solubility determination of drug in various Surfactants

Optimization of NLCs

Central composite designs are commonly used to analyze the influence of different variables on the properties of a drug delivery system. Table 2 represents the results of the measured responses (coded values) for Ranolazine-NLCs.

Table 2. Coded levels and measured responses for the 20-experiment formulation runs

F	X1	X2	X3	Y1	Y2	Y3	PDI	Zeta
1	1	4	10	294.53±1.23	49.38±0.28	52.13±0.22	0.564±0.02	-29.3±0.24
2	3	3	7.5	159.36±0.59	72.95±1.26	78.63±0.53	0.628±0.04	-24.1±0.13
3	5	4	5	268.37±0.24	61.52±0.42	68.59±0.41	0.354±0.03	-29.8±0.05
4	1	2	10	384.16±2.67	46.37±0.35	52.49±1.02	0.267±0.01	-20.5±0.22
5	1	4	5	314.92±6.52	51.36±0.82	61.49±1.16	0.298±0.01	-15.2±0.29
6	3	3	11.70	259.31±3.46	59.87±1.06	64.38±2.09	0.416±0.01	-28.4±0.25
7	3	3	7.5	143.26±8.21	74.11±1.29	78.46±1.07	0.328±0.12	-32.4±1.34
8	3	3	7.5	143.26±5.24	70.39±0.76	73.58±0.94	0.059±0.06	-26.9±2.06
9	3	1.31	7.5	186.74±2.97	65.49±0.58	67.43±1.36	0.097±0.04	-32.4±1.59
10	5	2	5	237.16±0.98	69.42±0.43	53.44±2.08	0.076±0.08	-33.8±0.52
11	5	2	10	294.36±3.51	62.38±1.04	80.21±0.64	0.099±0.12	-36.7±0.49
12	-0.36	3	7.5	369.51±2.69	46.29±1.06	42.36±0.59	0.268±0.09	-25.7±0.83
13	3	3	7.5	143.26±3.58	72.95±1.09	78.45±0.85	0.614±0.08	-29.1±0.25
14	1	2	5	243.15±8.61	63.82±1.25	69.35±1.34	0.584±0.06	-30.1±1.34
15	6.36	3	7.5	278.35±3.25	72.35±2.08	75.34±0.67	0.349±0.03	-28.2±3.26
16	3	3	7.5	184.39±2.93	72.95±4.03	65.38±2.09	0.526±0.04	-29.6±2.18

17	3	4.68	7.5	186.72±8.31	68.31±3.26	85.23±0.42	0.851±0.01	-30.4±1.09
18	5	4	10	126.49±5.46	85.34±1.29	92.37±0.31	0.287±0.06	-28.6±1.09
19	3	3	3.295	269.85±8.32	56.48±2.86	53.26±0.59	0.649±0.04	-29.1±2.05
20	3	3	7.5	143.26±2.67	72.95±2.38	69.83±0.24	0.427±0.07	-26.7±1.07

Figures 4, 5, and 6 exhibit three-dimensional response surface plots derived by fitting data to the polynomial equation. You may use these graphs to see how changing one or both of the other variables affects the answer when the third variable is held constant. For each answer, analyses of variance (ANOVA) were run to determine the statistical significance of the effects and interactions of X1X2, X2X3, and X1X3.

Effects of Variables on Mean Particle Size

The particle size of the formulations ranged from 143.26±2.67to 384.16±2.67 nm.

Size = +152.62 -33.95A -11.32 B +1.33C -14.85AB -25.66AC -45.06BC +61.68A2+ 13.17B2 +40.70C2

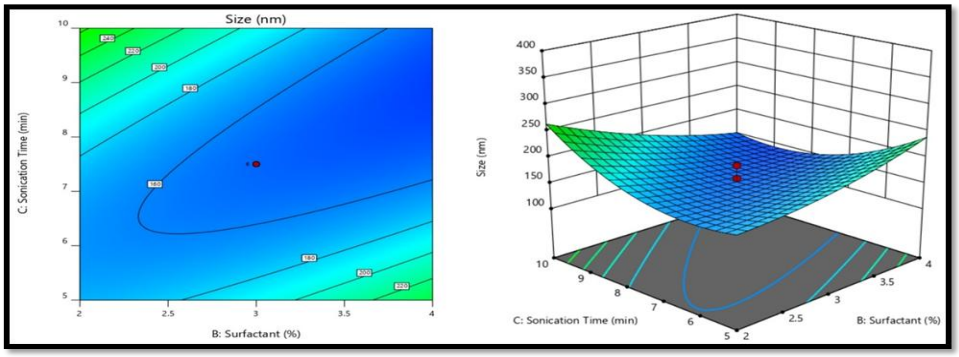

Figure 4: Response surface models showing the influence of the factors on the responses.

Effect of formulation variables on the percentage EE

The percentage of Ranolazine entrapped within the NLCs varied from 46.29±1.06% to 85.34±1.29%.

EE = +72.70 +8.17A +0.7581B +0.2234C +3.06AB +4.53AC -4.65A2 -1.97B2 -5.05C2

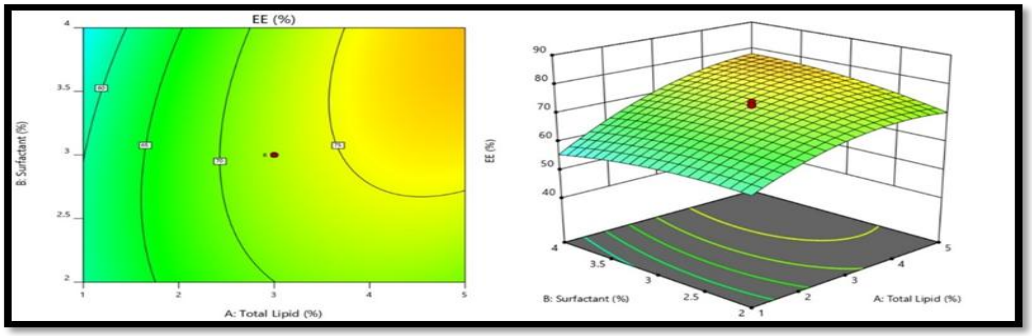

Figure 5: Response surface plots depicting the effect of the variables (AB) and the interaction between them on the response.

Effect of formulation variables on CDR

The CDR of the prepared NLCs ranged from 42.36±0.59to 92.37±0.31 (Table 2).

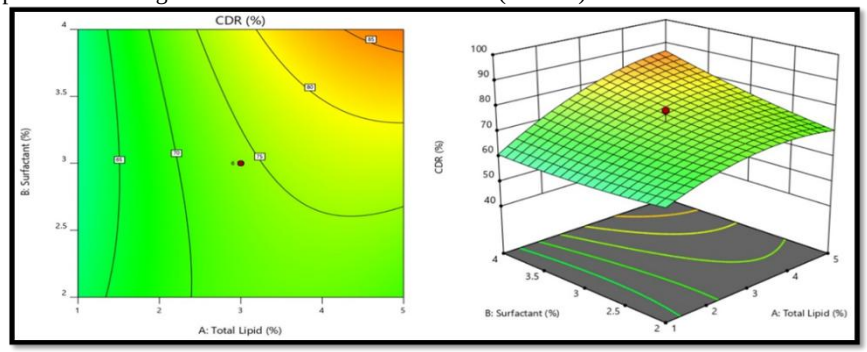

Figure 6: Three-dimensional surface plot for representing influence of the interaction of independent variables (AB)

Optimization and validation

The desire function technique was used to find the best formulation of ranolazine-NLCs. TheDesign Expert® 12.0.3.0 programme was used to create contour plots and a desirability plot. The optimum formulation was chosen with codedvalues of X1 (Total Lipid) and X2 (Surfactant concentration), respectively, from the desirability plot (Figure 7).

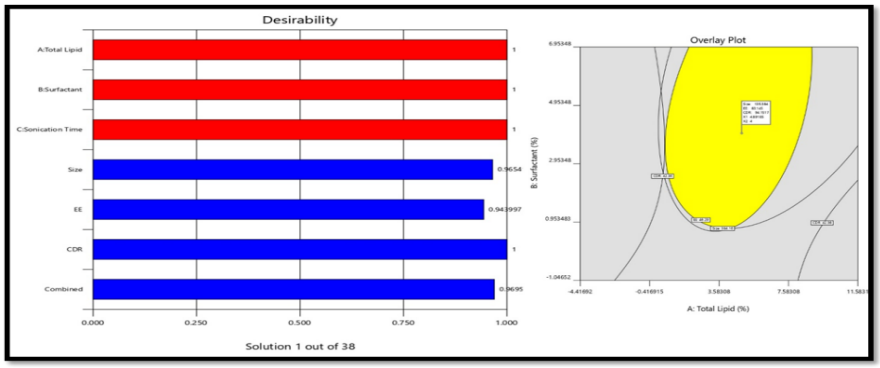

Figure 7: Desirability and Overlay plot showing the desirable region for selection of optimized Ranolazine-NLCs from CCD design

To verify the efficacy of the optimization method, a batch of optimised Ranolazine-NLCs (F18) was created using the specified values of independent variables from the overlayplot. In this study, we recorded both the expected and experimental values of the reactions and compared them. Non-significance ($p > 0.05$) was discovered for the percentage inaccuracy. The RSM model's reliability is demonstrated by the high degree of concordance between predicted and experimental results.

Particle size and zeta potential

The improved formulation's particle size and zeta potential data are depicted in Figure 8 A. The size distribution of ranolazine-NLCs was narrow and nanometric. (PDI 0.059±0.06) and an average diameter of 143.26±2.67 nm. Ranolazine-NLCs possessed a high zeta potential of -36.7±0.49mV (Figure 8 B).

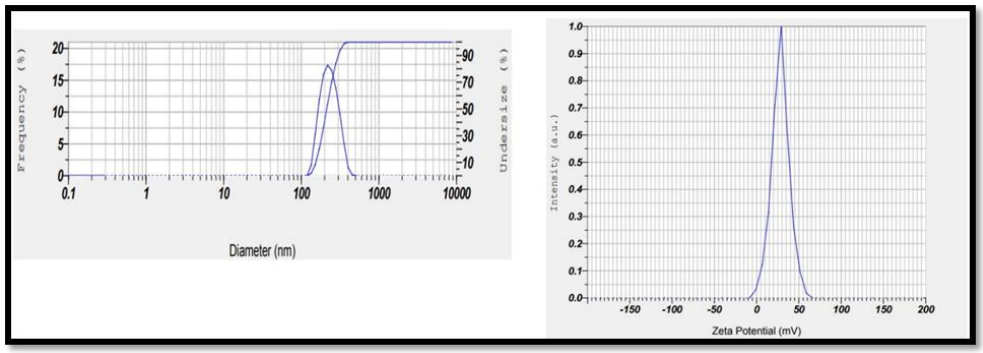

Figure 8: (A) Particle size and (B) Zeta potential of Ranolazine-NLCs

FTIR analysis

The FTIR spectrums of pure Ranolazine and Ranolazine-NLCs are presented in above Figure 9.

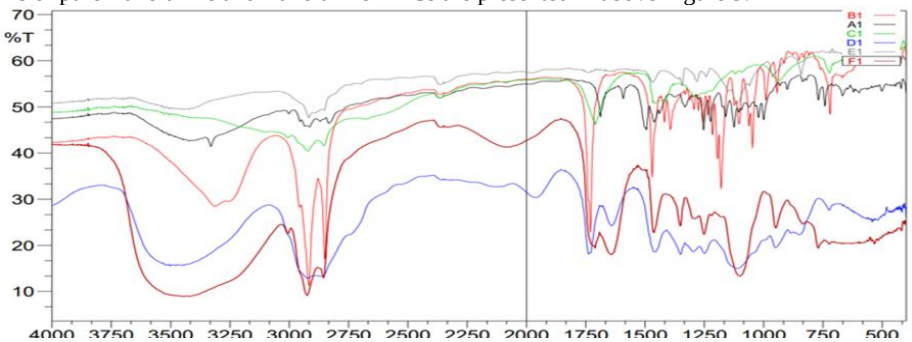

Figure 9: FTIR spectral studies of RZ-NLCs

Pure Ranolazine's infrared spectrum showed distinct peaks at 3328.40 cm 1 for NH- stretching, 1685.23 cm 1 for C=O stretching, 1591.33 cm 1 for C=O stretching of -COOH, 1296.18 cm 1 for C-N stretching, 1437.43 cm 1 for aromatic -

C=C stretching, 1459.49 cm 1 for -C=C stretching, and another peak at 1252.

DSC Study

Ranolazine and stearic acid reached endothermic peaks at 120.01°C and 77.09°C, respectively. Oleic acid and tween 80 displayed a melting point of 189.67°C and 51.33°C. The DSC analysis of poloxamer 188 and optimized NLCs showed 53.34°C, 95.48°C respectively.

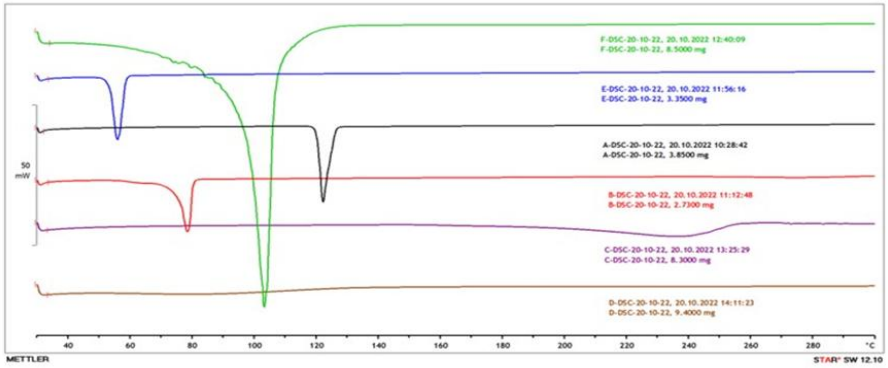

Figure 10: DSC thermogram of Pure Drug,

Surface Morphology of vesicles

SEM and TEM investigation, as shown in Figure 11, was used to completely characterise the morphology of NLCs in formulation F18.

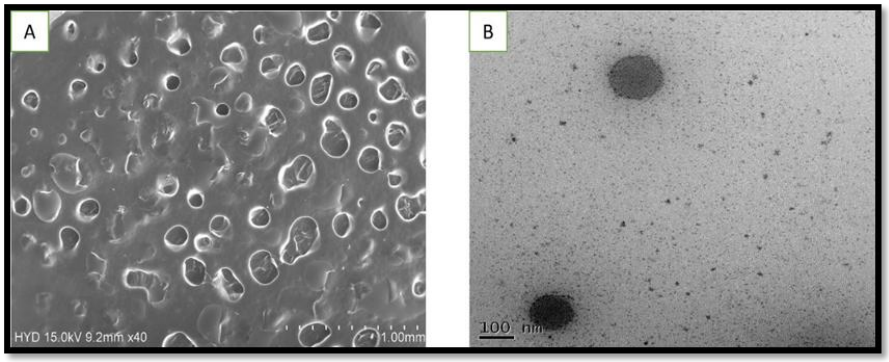

Figure 11: SEM &TEM of F18 displaying (A) its spherical structure, and (B) non-aggregating orientation.

In vitro drug release study

The in vitro release profiles of Ranolazine from freshly prepared and Ranolazine-NLCs and Ranolazine suspension in pH 1.2 and pH 7.4 were carried out in Franz diffusion cell and are presented in Figure 12 & 13. The cumulative percentage release from the freshly formulated Ranolazine NLCs (78.36%) and (47.83%) was less than that of freshly formulated Ranolazine suspension (96.26%) and (57.6%) in pH1.2 and pH 7.4 respectively.

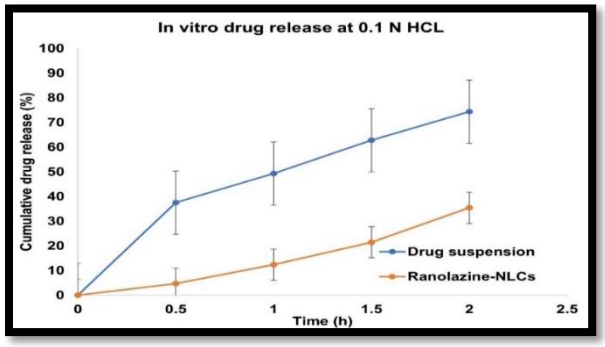

Figure 12: In vitro release of Ranolazine NLCs

formulations and drug suspension in pH1.2

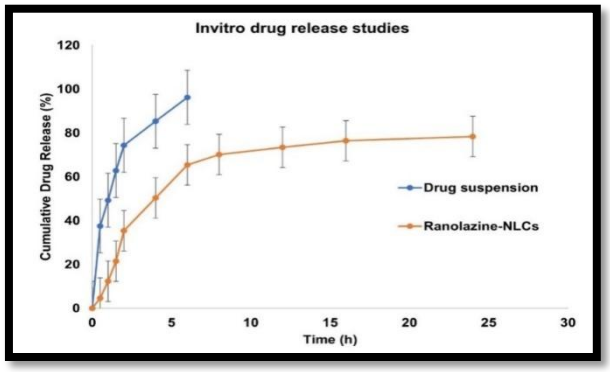

Figure 13: In vitro release of Ranolazine NLCs of formulations and Ranolazine drug suspension in pH 7.4.

Pharmacokinetic study

Figure 14 depicts the median plasma concentration-time profiles of Ranolazine following oral administration of drug solution and Ranolazine-NLCs. By employing the PK Solver programme, the pharmacokinetic parameters Cmax, tmax,

elimination rate constant (Ke), area under the curve (AUC) 0-t, (AUC) 0-∞ , and mean residence time (MRT) were determined, as shown in Table 3.

Table 3: Pharmacokinetic parameters of Drug suspension and Ranolazine NLCs

Pharmacokinetics Parameter	Drug Suspension	Optimized SLNs
C0 (mcg/ml)	0.969	1.892
K(hr-1)	0.031	0.0018
Dose (mg)	100	100
Vd (mL)	103172	52844.2
t1/2 (hr)	21.844	385.08
Clearance (L/hr)	3.273	0.0950
AUC 0-t (µg.h/mL)	0.367	0.598
AUC t-inf (µg.h/mL)	9.141	683.485
AUC Total (µg.h/mL)	24.495	718.24
MRT0-t (h)	34.56	43.126
C max(ng/mL)	1.93	5.689
T max (h)	3.46	4.35

Ranolazine-NLCs concentrations in plasma were consistently greater than those in medication solution. Ranolazine-NLCs had a peak concentration (Cmax) that was 2.4 times greater than drug solution. The AUC0-t and AUC 0-∞ for Ranolazine-NLCs were 3.03- and 3.5-folds higher than Ranolazine solution. There were statistically significant group differences in these pharmacokinetic parameters (p 0.001). The half-life of Ranolazine-NLCs was determined to be 12 hours, whereas that of Ranolazine solution was found to be 4 hours. Ranolazine-NLCs had a much higher MRT0- compared to Ranolazine solution, rising from 34.56 ± 5.85 to 43.126 ± 7.13 h, which indicate the prolonged residence time of Ranolazine-NLCs at the site of absorption.

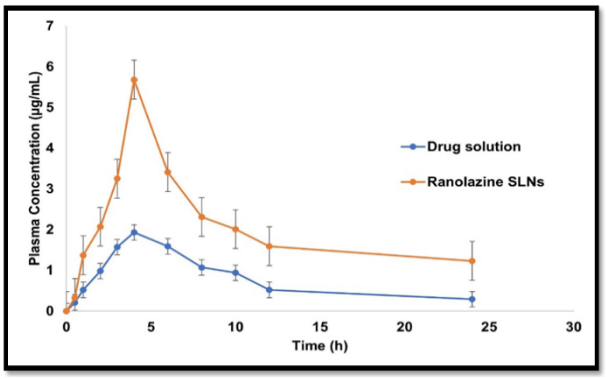

Figure 14: Plasma concentration vs. time curve of Ranolazine from Ranolazine solution and Ranolazine-NLCs

Pharmacodynamic study

Antihypertensive action was tested in vivo for 24 hours. The average systolic blood pressure of the animals in Group I was found to range between 152.36- and 173.58- mm Hg. Average systolic blood pressure dropped significantly (p 0.001) after 1 hour of oral delivery in groups II and III compared to group I (118.96±18.81 mm Hg and 124.38±8.4 mm Hg, respectively) (Figure15).

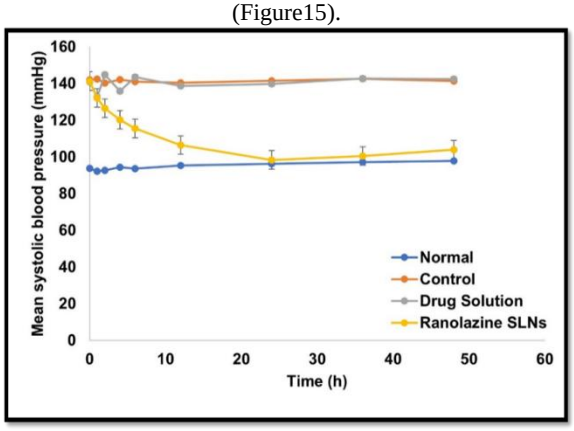

Figure 15. Animals were given 10 mg/kg of Ranolazine-NLCs, 10 mg/kg of Ranolazine solution, or normal saline to evaluate the antihypertensive effects in vivo. Summarized data (n=4) is presented as mean ±SD.

Additionally, for the whole 24-hour period, the mean systolic blood pressure of Ranolazine-NLCs was observed to be less than 130 mm Hg. Maximum blood pressure drop with ranolazine suspension was 135.6414.08 mm Hg, and this effect lasted for 4 hours until blood pressure began to rise again.

Stability studies of stored NLCs

All of the chosen NLCs formulations were tested for stability at 4 °C for three months, and the findings were reported in terms of mean particle size, particle distribution index, and zeta potential.

DISCUSSION

Liquid lipid i.e., oleic acid has showed highest solubilizing capacity toward Ranolazine. Amongst the used solid lipids, drugshowed thehighest solubility in stearic acid. The solubility of Ranolazine was found to be higher in Tween 80 than in other non-ionic surfactants and, therefore, it was selected as the surfactant for the NLCs formulation.

Effect on Particle Size

The PS of NLCs decreases significantly (p 0.05) when the concentration of lipids (factor A) increases in a design experiment. This is likely because of the intense homogenization pressure that so effectively disperses the lipids into their component parts. Likewise, it was discovered that raising the surfactant concentration (C) led to a concomitant drop in NLC PS. This may be because tween 80, when mixed with stearic acid, reduces both the system's viscosity and surface tension, leading to a reduced particle size of NLCs.

Effect onEE

An increase in drug EE within the NLCs is induced by raising the overall lipid and surfactant contents. Total lipid incorporation disturbs the solid lipid crystal arrangement, creating more room for drug molecules to fit. The hydrophobic interface of the scattered NLCs is typically covered by the molecules of the surfactant. High EE results from the drug molecules being partially absorbed into the

surfactant layer at the nanoparticles' surface at higher surfactant concentrations. A high concentration of tween 80 and surfactant likely enhanced the drug's solubility in the aqueous phase; as a result, the drug may have suffered partition from the NLCs to the aqueous medium, resulting in a reduction in EE%.

Effect on CDR

Antagonizing effects on the reaction Y3 were seen from the given interactions (X1X3) and (X2X3). This indicates that a reduction in PI and a preference for the formation of more uniformly dispersed nanoparticles are the results of increasing the quantity of Transcutol® in conjunction with an increase in either the oil or the surfactant concentration. By utilising a desirability function, we looked for the most effective way to construct Ranolazine-NLCs. Using Design Expert® 12.0.3.0, we were able to make a contour plot and a desirability plot. It was determined that the percentage of mistake was negligible and not statistically significant ($p > 0.05$). The RSM model was shown to be accurate due to the high degree of concordance between the calculated and measured values.

Figures 8A and 8B, respectively, provide the improved formulation's results on particle size and zeta potential. The solution might be clearer with smaller nanoparticles, which is thought to be a benefit of oral liquid formulations. Smaller particles with a lower PDI would also slow the pace at which they settled, allowing them to stay suspended in a solution. The significant negative zeta potential of ranolazine-NLCs demonstrated the stability of the nanoparticles. This is probably because particles reject one another, which reduces the propensity for aggregation.

The Ranolazine-NLCs' FTIR spectra revealed a distinctive, low-intensity peak of intact Ranolazine, confirming the absorption of Ranolazine into the lipid bilayer. Ranolazine-NLCs formulation's spectra showed a change in the peak intensities of pure drug, which confirms the drug's existence in the NLCs. The only significant change in the samples' DSC characteristic melting points was an expansion or contraction of the endothermic peak regions. This could have happened as a result of changes in the crystal structure brought on by the partial bulk drug's transition to a molten form as the temperature increased. The absence of the drug's endothermic peaks in NLCs, however, indicated that it was disseminated in the nanoparticles in a nanocrystalline form.

The spherical form and unilamellar structure of NLCs are seen in the SEM photos. Additionally, TEM pictures of the improved Ranolazine-NLC demonstrated that the particles had a limited size range, were non-aggregated, and were spherical in form. It was seen from various angles that the studied sample included only one type of colloidal species. The size determined by the PS analyzer and the average particle size shown in the TEM micrographs were in good agreement.

The biphasic pattern, burst or quick release at the beginning for a period of roughly 4 to 8 h, and sustained release up to 48 h were all visible in the in vitro release profiles of ranolazine from NLC's formulation. The drug molecules positioned on the surface of the nanocomposites cause the preliminary burst release of ranolazine from the ranolazine-NLCs. Because the combination of solid and liquid lipids functions as a reservoir for the NLCs and is lipophilic, there is sustained release of ranolazine. Ranolazine NLCs were freshly formulated at pH 1.2 and pH 7.4, respectively, and their cumulative percentage release was lower than that of freshly made Ranolazine solution. This might be explained by the surfactants on the NLCs' surface acting as a barrier to the diffusion of the medicinal moiety into the medium.

At every time point, the plasma concentrations of ranolazine-NLCs were greater than those of the drug solution. The P-gp efflux pump and hepatic first-pass metabolism contributed to the decreased Cmax and AUC values seen for ranolazine solution, whereas the addition of P-gp inhibitors such poloxamer 188 and Tween 80 in the nanometric formulation increased Cmax and AUC values. The results of the tmax demonstrated that the drug release from Ranolazine-NLCs was sustained, which is in line with the findings of in vitro release tests. The MRT0-∞ of ranolazine-NLCs was much higher than that of ranolazine solution, indicating that the ranolazine-NLCs had a longer residence time at the site of absorption. High AUC and MRT values of LGP-SLNs imply regulated drug administration by demonstrating an enhanced and sustained pharmacological action.

For 24 hours, in vivo antihypertensive action was carried out. It was discovered that group I animals were all hypertensive. After 1 hour of oral delivery, treatment groups II and III significantly reduced mean systolic blood pressure ($p< 0.001$) as compared to group I. (Figure 15). Furthermore, it was discovered that throughout the course of a 24-hour period, the mean systolic blood pressure in ranolazine-NLCs was less than 130 mm Hg. Maximum blood pressure lowering was seen with ranolazine suspension for 4 hours, and thereafter there was an increase. Results indicated that the oral administration of ranolazine is improved by the newly created formulation of ranolazine-NLCs.

NLCs formulation was discovered to be stable for the first two months, but after that point, a significant rise in the PDI (above 0.6) may have indicated the emergence of a polydisperse system with an aggregation propensity. Due to the inclusion of a sterically stabilising surfactant, the optimised Ranolazine NLCs had zeta potential values less than 30 mV yet adequate to achieve stable dispersions..

CONCLUSION

In order to create an optimal nanostructured lipid carrier formulation of ranolazine with increased oral bioavailability and GI stability, the systemic CCD technique was demonstrated in the current work. Excipients that are usually considered as safe were used in RZ-NLC development in quantities much below their Inactive Ingredients Guide limitations. RZ-NLC was successfully produced and refined and showed the following characteristics: nano size, uniform size distribution, high entrapment, prolonged release, and a noticeably improved oral bioavailability. As a result, the NLC formulation significantly increased the oral bioavailability of ranolazine and showed a potential future for the oral administration of medications with low water solubility.

REFERENCES:

i. M. Destro, P. Preti, A. D'Ospina, N.N. Christian Achiri, A.R. Ricci, F. Cagnoni, Olmesartanmedoxomil: recent clinical and

experimental acquisitions, Expert Opin. Drug Metab. Toxicol., 5 (2009) 1149-1157.

ii. H. Brunner, The new oral angiotensin II antagonist olmesartanmedoxomil: a concise overview, J. Hum. Hypertens., 16 (2002) S13-6.

iii. L.R. Schwocho, H.N. Masonson, Pharmacokinetics of CS- 866, a New Angiotensin II Receptor Blocker, in Healthy Subjects, J. Clin. Pharmacol., 41 (2001) 515-527.

iv. H. Théophile, X.-R. David, G. Miremont-Salamé, F. Haramburu, Five cases of sprue-like enteropathy in patients treated by olmesartan, Dig. Liver Dis., 46 (2014) 465-469.

v. S.E. Dreifuss, Y. Tomizawa, N.J. Farber, J.M. Davison, A.E. Sohnen, Spruelike enteropathy associated with olmesartan: an unusual case of severe diarrhea, Case Rep. Gastrointest. Med., 2013 (2013) 618071.

vi. S. Beg, G. Sharma, K. Thanki, S. Jain, O. Katare, B. Singh, positively charged self-nanoemulsifying oily formulations of olmesartanmedoxomil: systematic development, in vitro, ex vivo and in vivo evaluation, Int. J. Phar., 493 (2015) 466-482.

vii. M.J. Kang, H.S. Kim, H.S. Jeon, J.H. Park, B.S. Lee, B.K. Ahn, K.Y. Moon, Y.W. Choi, In situ intestinal permeability and in vivo absorption characteristics of olmesartanmedoxomil in self-microemulsifying drug delivery system, Drug Dev. Ind. Pharm., 38 (2012) 587-596.

viii. B. Gorain, H. Choudhury, A. Kundu, L. Sarkar, S. Karmakar, P. Jaisankar, T.K. Pal, Nano emulsion strategy for Olmesartanmedoxomil improves oral absorption and extended antihypertensive activity in hypertensive rats, Colloids Surf. B Biointerfaces, 115 (2014) 286- 294.

ix. Fathi HA, Allam A, Elsabahy M, Fetih G, El-Badry M. Nanostructured lipid carriers for improved oral delivery and prolonged antihyperlipidemicefect of simvastatin. Colloids Surf B Biointerfaces. 2017; 162:236–45.

x. Porter CJH, Trevaskis NL, Charman WN. Lipids and lipid-based formulations: optimizing the oral delivery of lipophilic drugs. Nat Rev Drug Discov. 2007; 6:231–48.

xi. Lupo E, Locher R, Weisser B, Vetter W. In vitro antioxidant activity of calcium antagonists against LDL oxidation compared with α-tocopherol. Biochembiophys res commun. 1994;203(3):1803–8.

xii. Godfraind T. Antioxidant efects and the therapeutic mode of action of calcium channel blockers in hypertension and atherosclerosis. Philos Trans R SocLond B BiolSci. 2005; 360:2259–72.

xiii. Amasya G, Aksu B, Badilli U, Onay-Besikci A, Tarimci N. QbD guided early pharmaceutical development study: production of lipid nanoparticles by high pressure homogenization for skin cancer treatment. Int J Pharm. 2019; 563:110–21.

xiv. Shrestha N, Bouttefeux O, Vanvarenberg K, Lundquist P, Cunarro J, Tovar S, Khodus G, Andersson E, Keita AV, Dieguez CG, Artursson P, Preat V, Beloqui A. Stimulation of GLP-1 secretion and delivery of GLP-1 agonists via nanostructured lipid carriers. Nanoscale. 2018;10(2):603–13.

xv. Shete H, Patravale V. Long chain lipid-based tamoxifen NLCS. Part I: preformulation studies, formulation development and physicochemical characterization. Int J Pharm. 2013; 454:573–584.

xvi. D'Souza S, Faraj JA, Giovagnoli S, DeLuca PP. IVIVC from long acting olanzapine microsphere. Int J Biomat. 2014;1–12.

xvii. Qadri GR, Ahad A, Aqil M. Invasomes of isradipine for enhanced transdermal delivery against hypertension: formulation, characterization, and in vivo pharmacodynamic study. Artif cells nanomedbiotechnol. 2017;45(1):139–45.

xviii. Ohkawa H, Ohishi N, Yagi K. Assay for lipid peroxides in animal tissues by thiobarbituric acid reaction. Anal Biochem. 1979;95(2):351–8.

xix. Pogodina M, Shornikova YS, ChentsovluS. Electron microscopy description of cardiomyocytes from the left ventricle of rat heart after apoptosis induction by isoproterenol. Biol Bull. 2006;33(1):19–29.

xx. Kaithwas V, Dora CP, Kushwah V, Jain S. Nanostructured lipid carriers of Olmesartanmedoxomilwithenhanced oral bioavailability. Colloids Surf B Biointerfaces. 2017; 154:10–20.

xxi. Alam T, Khan S, Gaba B, Haider MF, Baboota S, Ali J. Adaptation of quality by design-based development of isradipinenanostructured lipid carrier and its evaluation for in vitro gut permeation and in vivo solubilization fate. J Pharm Sci. 2018;107(11):2914–26.

xxii. Severino P, Santana MHA, Souto EB. Optimizing SLN and NLCS by 22 full factorial design: efect of homogenization technique. Mater SciEng C. 2012; 32:1375–9.

xxiii. Subedi RK, Kang KW, Choi HK. Preparation and characterization of solid lipid nanoparticles loaded with doxorubicin. Eur J Pharm Sci. 2009; 37:508–13.

xxiv. Shah B, Khunt D, Bhatt H, Misra M, Padh H. Intranasal delivery of venlafaxine loaded nanostructured lipid carrier: risk assessment and QbD based optimization. J Drug DelivSciTechnol. 2016; 33:37–50.

xxv. Jawahar N, Hingarh PK, Arun R, Selvaraj J, Anbarasan A, Sathianarayanan S, Nagaraju G. Enhanced oral bioavailability of an antipsychotic drug through nanostructured lipid carriers. Int J BiolMacromol. 2018; 110:269–75.

xxvi. Attari Z, Bhandari A, Jagadish PC, Lewis S. Enhanced ex vivo intestinal absorption of Olmesartanmedoxomilnanosuspension: preparation by combinative technology. Saudi Pharm J. 2016; 24:57–63.

xxvii. L. A. Cubillos-Garzon, J. P. Casas, C. A. Morillo, L. E. Bautista, Congestive heart failure in latinamerica: The next epidemic, Am Heart J 147 (2004) 412-417.

xxviii. P. M. Kearney, M. Whelton, K. Reynolds, P. Muntner, P. K. Whelton, J. He, Global burden of hypertension: Analysis of worldwide data, Lancet 365 (2005) 217-223.

xxix. N. Campbell, E. R. Young, D. Drouin, B. Legowski, M. A. Adams, J. Farrell, J. Kaczorowski, R. Lewanczuk, M. Moy Lum-Kwong, S. Tobe, A framework for discussion on how to improve prevention, management, and control of hypertension in canada, Can J Cardiol 28 (2012) 262-269.

xxx. A. Ahad, A. M. Al-Mohizea, F. I. Al-Jenoobi, M. Aqil, Transdermal delivery of angiotensin ii receptor blockers (arbs), angiotensin-converting enzyme inhibitors (aceis) and others for management of hypertension, Drug Deliv 23 (2016) 579- 590.

xxxi. Y. Cao, L. L. Shi, Q. R. Cao, M. Yang, J. H. Cui, In-vitro characterization and oral bioavailability of organic solvent-free solid dispersions containing telmisartan, Iran J Pharm Res 15 (2016) 385-394.

xxxii. L. Yang, Y. Shao, H. K. Han, Improved ph-dependent drug release and oral exposure of telmisartan, a poorly soluble drug through the formation of drugaminoclay complex, Int J Pharm 471 (2014) 258-263.

xxxiii. P. Lepek, W. Sawicki, K. Wlodarski, Z. Wojnarowska, M. Paluch, L. Guzik, Effect of amorphization method on telmisartan solubility and the tableting process, Eur J Pharm Biopharm 83 (2013) 114-121.

xxxiv. S. M. Moghddam, A. Ahad, M. Aqil, S. S. Imam, Y. Sultana, Optimization of nanostructured lipid carriers for topical delivery of nimesulide using box-behnken design approach, Artif Cells NanomedBiotechnol (2016) 1-8.

xxxv. R. H. Muller, M. Radtke, S. A. Wissing, Solid lipid nanoparticles (sln) and nanostructured lipid carriers (nlc) in cosmetic and dermatological preparations, Adv Drug Deliv Rev 54 Suppl 1 (2002) S131-155.

xxxvi. S. Khan, S. Baboota, J. Ali, R. S. Narang, J. K. Narang, Nanostructured lipid carriers: An emerging platform for improving oral bioavailability of lipophilic drugs, Int J Pharm Investig 5 (2015) 182-191.

xxxvii. Bas D, Boyaci IH. Modeling and optimization I: usability of response surface methodology. J Food Eng. 2007; 78:836-845.

xxxviii. Zhen HE, Xu-tao Z and Gui-qing X. Product quality improvement through response surface methodology: a case study. Presented during the Proceedings of 2013 International Conference on Technology Innovation and Industrial Management: Phuket, Thailand; May 2013: S4-120-130.

xxxix. Shah MK, Madan P, Lin S. Preparation, in vitro evaluation and statistical optimization of carvedilol-loaded solid lipid nanoparticles for lymphatic absorption via oral administration. Pharm Dev Technol. 2014;19(4):475-485.

xl. Javed MN, Kohli K, Amin S. Risk assessment integrated QbD approach for development of optimized bicontinuousmucoadhesivelimicubes for oral delivery of rosuvastatin. AAPS PharmSciTech. 2018;19(3):1377-1391.